Carbohydrate Polymers 99 (2014) 356–364

Contents lists available at ScienceDirect

Carbohydrate Polymers

journal homepage: www.elsevier.com/locate/carbpol

Quaternized and sulfated xylan derivative films

Ivan Šimkovic[a,*], Adam Tracz[b], Ivan Kelnar[c], Iveta Uhliariková[a], Raniero Mendichi[d]

[a] Institute of Chemistry, Slovak Academy of Sciences, 845 38 Bratislava, Slovakia
[b] Centre of Molecular and Macromolecular Studies, Polish Academy of Sciences, 90-393 Lodz, Poland
[c] Institute of Macromolecular Chemistry, Academy of Sciences of the Czech Republic, Heyrovsky Square 2, 162 06 Prague, Czech Republic
[d] Istituto per lo Studio delle Macromolecole (CNR), Via E. Bassini 15, 20133 Milan, Italy

ARTICLE INFO

Article history:
Received 15 July 2013
Received in revised form 22 August 2013
Accepted 23 August 2013
Available online 28 August 2013

Keywords:
Xylan
Films
Composites
Mechanical testing
Thermal properties

ABSTRACT

Xylan quaternized sulfate films were prepared from beech xylan (X) and compared with fully sulfated xylan films (XS). When quaternized xylan (QX) was prepared in the first step (DS_Q = 0.55), than by sulfation of QX in the second step the fully substituted ampholytic derivative (QXS; DS_Q = 0.33; DS_S = 1.67) could be obtained. By sulfation in first step, xylan sulphate (SX, DS_S = 0.70) was obtained and by subsequent quaternization, SXQ film with DS_Q = 0.55 and DS_S = 0.33 which contained partially unsubstituted hydroxyls. The molar masses (M_n) of the film's soluble parts were increasing in order X < SX < SXQ < QX < XS < QXS. In all films there were some insoluble particles present as determined by the amount of recovered masses by SEC-MALS. The materials were further characterized by AFM, XRD, TG/DTG/DTA, NMR and mechanical testing. QXS and SXQ could form mechanically more stable films than XS specimens.

1. Introduction

Composites and especially films from all-polysaccharide composites (Šimkovic, 2013) are increasing its importance due to ecological aspects and interesting properties. Also xylan-containing films were intensively studied (Deutschmann & Dekker, 2012; Grondahl, Erisson & Gatenholn, 2004; Hansen & Plackett, 2008; Mikkonen et al., 2012; Peng, Ren, Zhang & Sun, 2011; Šimkovic, Gedeon, Uhliariková, Mendichi & Kirschnerová, 2011a,b; Šimkovic, 2008; Zhang & Whistler, 2004). Their applications are dependent upon their properties. Partially water soluble films could be used for covering the surfaces of food, pharmacological and other products to prevent drying or oxidative changes. Their mechanical and optical properties are dependent upon molar mass, presence of ion-exchanging groups and water solubility.

The use of scanning electron microscopy (SEM) in previous studies allowed us to make conclusions about the homogeneity of the film surface as well as on the break. When broken the film is mechanically destroyed its structure could be observed on the fracture from inside (Šimkovic et al., 2011a,b). With the use of atom force microscopy (AFM) besides better enlargement also the third dimension of the surface could be observed at the nanometre scale. We also used SEC-MALS, XRD, mechanical tester, solution and solid state NMR spectroscopy and thermal analysis (TG/DTG/DTA) to characterize the samples. This data made it possible to understand the relation between chemical structure, type of substituent, molar mass and water solubility together with the effect of chemical modification on homogeneity of the surface, tensile strength of the films and thermal properties of the material.

2. Experimental

2.1. Materials

Xylan (X) was extracted from beech sawdust holocellulose with 10% NaOH analogous to that described for hornbeam wood (Ebringerova et al., 1969). According to ^{1}H NMR anomeric signals integration of the soluble part at 60 °C in 100 atom% D_2O (ARMAR Chemicals), the sample contained 16.67% of 4-O-methyl-D-glucuronic units and 83.33% of xylose. The sonicated fraction (132 kHz, 129 W, 18 × 10 min at 50 °C, WX) had M_n = 3.8 kg/mol and D = 2.0 according to SEC-MALS analysis (see Section 2.2) 64.2% of sample mass was recovered. Sulphur trioxide pyridine complex (Py·SO_3, Aldrich) and all other chemicals used were of commercial grade and were not further purified.

Quaternized xylan (QX) was prepared by mixing X (1.654 g; 10 mmol) with glycidyltrimethylammonium chloride (GTMAC; 4.47 ml, 20 mmol; 60% solution) and water (17 ml; 1 mol in total), containing NaOH (1.6 g, 20 mmol). After stirring (500 RPM) at 60 °C for seven hours the reaction was stopped by dilution and adjusted to pH 5.0 with HCl and dialyzed using 10–12 kDa molar mass cut-off dialysis tubing (SERVA # 44126). After preconcentration

* Corresponding author. Tel.: +421 2 59410289; fax: +421 2 59410222.
E-mail address: chemsimk@savba.sk (I. Šimkovic).

0144-8617/$ – see front matter © 2013 Elsevier Ltd. All rights reserved.
http://dx.doi.org/10.1016/j.carbpol.2013.08.075

on vacuum evaporator (35 °C; 3.3–4 kPa) the solution was cast on Petri dish and dried at room temperature (RT) to prepare film (QX, 1.8574 g; N, 1.93; C, 40.49; H, 6.94; DS_Q = [nitrogen content (%)/nitrogen content of fully substituted anhydroxylose (%)] × 2 = 0.55; yield = [theoretical yield at obtained DS/amount of X used] × 100 = 69%).

In the second step QX (0.9287 g; 5 mmol) was mixed with DMSO (35.51 ml; 500 mmol) and frozen overnight. Subsequently Py·SO_3 complex (9.5496 g; 60 mmol) was added and reaction was run for ten hours at 60 °C/500 RPM. The mixture was precipitated in 96% ethanol (600 ml) saturated with $CH_3COONa{\cdot}3H_2O$ (31.5 g) and the separated precipitate solubilized in water and dialyzed. After preconcentration on vacuum evaporator and adjustment of pH to 9 the solution was cast on Petri dishes and dried at RT to constant weight (QXS, 1.6284 g; N, 1.16; DS_Q = 0.33; C, 24.64; H, 4.15; S, 15.91; DS_S = [sulphur content (%)/sulphur content of fully substituted anhydroxylose (%)] × 2 = 1.67; yield = 97%).

The fully sulfated xylan (XS) was prepared by mixing xylan (1.654 g; 10 mmol) with DMF (38.72 ml; 500 mmol) containing Py·SO_3 complex (7.958 g; 50 mmol) and subsequent stirring (500 RPM) at 60 °C for 12 h and worked up as above (2.4483 g; S, 19.00; C, 16.11; H, 3.02; DS_S = 2.0; 73% yield).

Partially sulfated xylan SX was obtained under analogous conditions at molar ratio of xylan/DMF/Py·SO_3 complex = 10/500/25 when the experiment was run for only 6 h (SX; 1.624 g; C, 28.34; H, 4.99; S, 6.66; DS_S = 0.70; 84% yield). When part of the SX sample (1.2242 g; 5 mmol) was quaternized by dissolving in 15.98 ml of water (1 mol in total) containing 1.6 g NaOH (40 mmol) using 4.48 ml of GTMAC (20 mmol) and treated under analogous conditions as above SXQ (0.7471 g; N, 1.95; DS_Q = 0.55; C, 38.49; H, 6.04; S, 3.16; DS_S = 0.33) film was prepared.

2.2. Analytical methods

Solution NMR measurements were performed as described previously (Šimkovic et al., 2011a). The elemental composition of specimens was performed on Macro Analyzer (Elementar Analysensystem GmbH, Donauestr, 7, 63452 Hanau, Germany) at detection ranges for C: 0–150 mg (or 100%); H: 0–15 mg (or 100%); N: 0–100 mg (or 100%) and S: 0–18 mg (or 100%).

SEC-MALS characterization was performed using 0.1 M carbonate buffer at pH 10.0 as SEC mobile phase (two TSK gel columns; G4000 and G3000; Tosoh Bioscience; at 35 °C; flow rate: 0.8 mL/min; dn/dc = 0.146 g/ml; sample concentration: 3 mg/ml).

For AFM analysis the films were dissolved in deionized water with the help of ultrasound (1 h at 60 °C) and obtained a solution which was then filtered through 0.8 μm filter. The films were prepared by casting the obtained solution on glass and drying at 60 °C. Morphological investigations were performed using Nanoscope IIIa AFM microscope (Digital Instruments/Veeco, Santa Barbara, CA), operated in tapping mode. Rectangular silicon cantilevers of model RTESP (Veeco Instruments) were used throughout the study. All scans were performed in air, at room temperature. Height and phase contrast images were recorded simultaneously with a scan frequency below 2 Hz.

For mechanical testing, dog-bone specimens (type B, ISO 527–2) with 10 mm length of the working part were cut. Tensile tests were carried out at 22 °C using an Instron 5800 apparatus at a crosshead speed of 1 mm/min. At least eight specimens were tested for each sample. The stress-at-break (σ_b), elongation-at-break (ε_b) and Young's modulus (E) were evaluated.

Wide-angle X-ray diffraction (WAXS) patterns were obtained with a powder diffractometer HZG/4A (Freiberger Präzisionsmechanik GmbH, Germany) and monochromatic CuKα radiation.

Solid state NMR experiments were performed on multinuclear 400 MHz Varian spectrometer operating at 100.54 MHz frequency for ^{13}C NMR experiments and equipped with 4 mm T3-HXY probe working at 10 kHz spinning rate; spin-lattice relaxation time T_1 = 240 s for 1024 scans. The sample of measured xylan was in lyophylized form (~50 mg).

TG/DTG/DTA measurements were run on NETSCH STA 449F3 STAF3A-0382 instrument using air environment (50 ml/min) and nitrogen for balance maintenance (PG = 20 ml/min). The sample amounts used were ~30 mg cuts from the films prepared. The heating rate was 10 K/min in Al_2O_3 crucibles.

3. Results and discussion

3.1. Order of chemical modification

According to elemental analysis by quaternization of X at X:NaOH:GTMAC:H_2O = 10/20/20/1000 molar ratio, the trimethylammonium-2-hydroxypropyl- (TMAHP) group was introduced (DS_Q = 0.55), and in this way positively charged film QX was prepared in the first step. When sulfated in the second step in DMSO (QX:DMSO:Py·SO_3 = 5/500/60) the fully substituted QXS derivative with DS_Q = 0.33 and DS_S = 1.67 was obtained. When X was sulfated in DMF with Py·SO_3 complex at 10/500/50 molar ratio, fully substituted xylan sulfate (XS) was prepared. When the ratio was changed to 10/500/25 the DS_S of the product (SX) was only 0.70. By subsequent quaternization of SX at SX:NaOH:GTMAC:H_2O = 5/40/20/100, SXQ film with DS_Q = 0.55 and DS_S = 0.33 was prepared. The decrease of DS_S indicates that some desulfation took place due to NaOH presence. The NMR data of QX, SX, QXS, and SXQ are listed in Table 1.

According to integration of anomeric protons of QX, DS_Q = 0.32 and 16% of xylose units are substituted with 4-O-methyl-D-glucuronate (MeGlcA) units. The chemical shifts of TMAHP-group [55.04/3.22 ppm –N(CH_3)$_3$; 69.20/3.48 ppm –CH_2N; 65.97/4.39 ppm –CHOH; 74.85/3.71, 3.83 ppm –O–CH_2] as well as all the data listed were obtained by 2D experiments (see Section 2). According to heteronuclear multiple bond correlation (HMBC) experiment the signal of –O–CH_2– (3.71 ppm) of the TMAHP-group is in correlation with *C-2* of quaternized xylose unit at 82.34 ppm (Table 1). This indicates that the xylose unit is substituted with quaternary group at C-2 position. Also the difference in chemical shifts of H-2/C-2 atoms of that unit in relation to the values of unsubstituted internal xylose unit confirs the hypothesis.

The partially sulfated sample (SX; Table 1) has almost identical chemical shifts of unsubstituted units observed on QX and also the substituents at H-2/C-2 and H-3/C-3 have dramatically different chemical shift than analogous values for non-substituted xylose units. It also contained 4-O-methyl-D-glucuronic acid units attached to C-2 of 11% of xylose units. Beside those two types of substituents also additional hexose anomeric signal 5.04/92.44 ppm was observed in correlation with signals at 3.90/75.70, 4.26/69.34, 4.00/67.36 ppm and CH_2 group with signals at 3.98, 3.84/61.92 ppm. According to literature it might be related to sulfated cellulose at C-6 (Wang, Li, Zheng, Normakhamatov, & Guo, 2007). This result indicates the presence of cellulose impurities in the used X sample.

The fully substituted QXS was predominantly sulfated at C-3 and the rest of the free C-2 positions of D-xylose units. It did not contain 4-O-methyl-D-glucuronic acid units. Additionally probably all hydroxyls of the TMAHP-groups were sulfated which dramatically affected the NMR data by changing the chemical shifts of hydroxyls of the TMAHP-substituent and both types of quaternized groups are observed. For non-sulfated substituents the shifts were at 3.22/55.08 ppm for N(CH_3)$_3$; 3.49/69.21 ppm for –CH_2N group; and 4.38/65.93 ppm for –CH(OH)– group, while the –O–CH_2– group could not be assigned. On sulfated

Table 1
NMR data of samples (ppm).

Sample/unit	H_1/C_1	H_2/C_2	H_3/C_3	H_4/C_4	H_5/C_5	H_6/C_6	OCH_3
QX/MeGlcA	5.26/98.25	3.59/72.31	3.76/72.99	3.27/83.06	4.29/73.14	–/177.06	3.48/60.45
QX/Xyl[a]	4.64/101.92	3.47/77.37	3.66/73.86	3.81/76.93	3.42[b]/63.72	–	–
QX/Xyl[c]	4.48/102.42	3.32/73.43	3.57/74.43	3.79/77.20	3.40[b]/63.72	–	–
QX/Xyl[d]	4.57/102.11	3.20/82.34	3.65/73.86	3.80/77.37	3.39[e]/63.72	–	–
SX/MeGlcA	5.26/98.40	3.58/72.28	3.77/73.13	3.26/83.13	4.29/73.20	–/177.27	3.47/60.47
SX/Xyl[a]	4.63/102.11	3.47/77.49	3.65/73.21	3.80/76.81	3.40[e]/63.60	–	–
SX/Xyl[c]	4.48/102.50	3.31/73.53	3.57/74.53	3.79/77.25	3.39[e]/63.83	–	–
SX/Xyl[f]	4.73/100.37	4.06/80.03	3.85/n.a.[g]	n.a.[g]	3.48[h]/n.a.[g]	–	–
SX/Xyl[i]	4.67/101.11	3.62/71.51	4.40/79.77	3.97/73.68	3.52[j]/62.01	–	–
QXS/Xyl[c]	4.53/102.04	3.36/73.32	3.60/74.20	3.84/76.85	3.42[k]/63.21	–	–
QXS/Xyl[d]	n.a.[g]	3.19/82.40	n.a.[g]	n.a.[g]	n.a.[g]		
QXS/Xyl[f]	4.72/100.74	4.06/80.29	n.a.[g]	n.a.[g]	n.a.[g]		
QXS/Xyl[i]	4.67/101.09	3.60/71.64	4.41/80.13	3.96/73.86	3.54[l]/62.04	–	–
QXS/Xyl[m]	5.08/97.19	4.38/72.98	4.74/73.09	4.01/72.95	3.81[n]/58.80	–	–
SXQ/MeGlcA	5.28/98.42	3.58/72.25	3.77/72.95	3.29/82.36	4.29/73.20	–/n.a.[g]	3.49/60.80
SXQ/Xyl[c]	4.49/102.51	3.31/73.55	3.57/74.42	3.79/77.13	3.41[b]/63.68		
SXQ/Xyl[d]	4.58/102.24	3.18/82.37	3.64/74.19	3.81/77.22	3.38[b]/63.64		
SXQ/Xyl[i]	4.70/100.98	3.67/n.a.[k]	n.a.[k]	3.98/73.84	3.50[b]/60.97		

[a] Xyl unit substituted with MeGlcA unit.
[b] H_{ax} of CH_2 with H_{eq} at 4.12 ppm.
[c] Non-substituted Xyl unit.
[d] Xyl unit substituted with quaternary group at C-2.
[e] H_{ax} of CH_2 with H_{eq} at 4.11 ppm.
[f] Xyl unit substituted with sulfate group at C-2.
[g] Not assigned.
[h] H_{ax} of CH_2 with H_{eq} at 4.16 ppm.
[i] Xyl unit substituted with sulfate group at C-3.
[j] H_{ax} of CH_2 with H_{eq} at 4.21 ppm.
[k] H_{ax} of CH_2 with H_{eq} at 4.14 ppm.
[l] H_{ax} of CH_2 with H_{eq} at 4.20 ppm.
[m] Xyl unit substituted with sulfate group at C-2 and C-3.
[n] H_{ax} of CH_2 with H_{eq} at 4.34 ppm.

TMAHP-group the values were: 3.25/55.08 ppm for $N(CH_3)_3$ group; 3.78/67.62 ppm for $-CH_2N$ group; 4.96/73.00 ppm for $-CH(OSO_3Na)$ group and 4.11/71.97 ppm for $-O-CH_2-$ group. For QXS sample beside partially sulfated signals of xylose units substituted either at C-2 or C-3 position also fully substituted xylose units were identified (Table 1). Also for QXS samples some additional modified cellulose sulfates were observed but with different chemical shifts than analogical signals observed on SX sample. Also for this sample not all the signals could be assigned.

The SXQ sample contained sulfate groups only in the C-3 position (Table 1), which could be explained by partial desulfation during the quaternization process in the second step. Also in this case some cellulose sulfate components were observed. This sample contained 7% of 4-O-methyl-D-glucuronic acid units linked to C-2 of xylose units.

3.2. SEC-MALS analysis

Results in Table 2 indicate the effect of chemical modification on solubility of the product as well as on molar masses. When the film prepared from X was characterized by SEC-MALS, its numerical number average molar mass (M_n) was the smallest from all studied samples with the biggest polydispersity (M_w/M_n) and the smallest amount of recovered mass. By the chemical modification the solubility of samples increased, which is represented by increased values of recovered mass. Also the polydispersity of obtained samples decreased in comparison to the starting material. XS film had the second lowest polydispersity from all studied samples, although it contained the second biggest amount of insoluble mass. SX had the second lowest M_n from all studied samples and the biggest polydispersity from all modified samples. SXQ formation resulted in decrease of polydispersity. The quaternization in the first step resulted in the highest solubility of QX from all studied samples. By subsequent sulfation of QX in DMSO QXS with the smaller polydispersity value was obtained. So the M_n values of samples increased in order X < SX < SXQ < QX < XS < QXS, while the weight molar mass (M_w) values were increasing in order QX < SXQ < XS < SX < X < QXS. Due to the fact that SXQ and QXS contain oppositely charged ion-exchanging groups they probably form aggregates which affect the values of determined molar masses.

Table 2
SEC–MALS characterization of samples at pH 10.0.

Sample	M_p (1) [kg/mol]	M_p (2) [kg/mol]	M_n [kg/mol]	M_w [kg/mol]	M_w/M_n	Recovered mass [%][a]
X	521.0	6.2	4.0	45.3	11.34	12.2
XS	–	41.7	27.0	35.7	1.32	45.6
SX	850.0	29.2	9.3	39.1	4.18	71.5
SXQ	–	20.8	10.0	21.4	2.13	71.2
QX	–	21.8	10.4	17.2	1.66	75.8
QXS	–	65.9	47.3	57.8	1.22	61.3

[a] "Recovered mass" is the mass of sample (g) eluting (i.e. recovered) from the SEC columns, expressed as % of the sample injected mass (sample concentration times injection volume). The recovered mass is calculated from the area of the DRI concentration detector after accurate calibration.

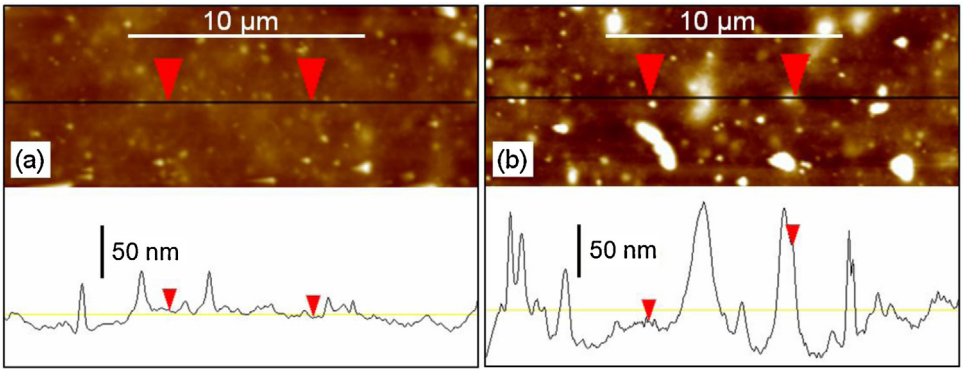

Fig. 1. AFM height images of xylan film prepared from solution: (a) filtered through 0.8 μm filter and (b) not filtered.

3.3. AFM analysis

There are insoluble particles observed on the AFM images of X, presented on Fig. 1a and b. They could be identified as white spots. This is concluded from the fact that these spots are much smaller on Fig. 1a when the sample was filtered through 0.8 μm filter. The filtered sample has much smoother surface as could be seen from section analysis, but some insoluble particles which passed through the filter are present on the surface. The insoluble components could not be eliminated even by sonication of solution prior film preparation (Fig. 2), but the surface of the film is much smoother than on unsonicated filtered sample on Fig. 1a. Similar images of bamboo xylan films were observed before (Peng et al., 2011).

The insoluble particles in the form of white aggregates were present in more compact forms distributed on the surface of quaternized xylan sample (QX; Fig. 3). According to section analysis it could be seen that the part of the flake-like structure crossed by the line was only about 5 nm high. This surface is much smoother than that of X.

The fully sulfated film XS (Fig. 4) contained on the surface also insoluble particles but with different shape than those of X or QX although their dimensions were similar. When the xylan sample was only partially sulfated (SX) and analyzed in a similar way, there were some pits on the surface (Fig. 5). They were up to 20 nm deep as could be seen on the section analysis. Pits were also visible on SEM image, but could not be distinguished from nodules or aggregates (Šimkovic, Gedeon, Uhliariková, Mendichi, & Kirschnerová, 2011b). The variation in surface profile might be caused by difference in the polysaccharide chains orientation inside the film. The smoothness of the surface is on the level of starting material (X), but the shape is different and more regular.

On SXQ sample (Fig. 6a), slightly different image was obtained with less smooth surface than on QX (Fig. 3), but much smoother than for SX (Fig. 4). The insoluble particles are remaining on the surface but their shape has changed with surface differences up to 50 nm. Image of QXS specimen (Fig. 6b) has much higher irregularities of the surface than SXQ sample with rods up to 100 nm high. So according to the vertical surface differences expressed in nanometers the smoothness of the surface is increasing in order: X = QXS (100 nm) < SXQ (50 nm) < SX (20 nm) < XS = QX (10 nm).

3.4. Mechanical properties

From the results in Table 3 it is obvious that modulus values of all modified samples were reduced in comparison with X, which indicates that modifications bring radical change also in supramolecular structure of xylan and interactions between its macromolecules. The most significant reduction in E for QX, which is accompanied with the biggest elongation indicates that quaternization under alkaline conditions most probably reduces interactions between X chains (enhances their compliance). Additionally, by quaternization in water/NaOH solution more material could be solubilized as observed by SEC-MALS analysis. All the values of stress at the break (σ_b) obtained on modified samples are smaller than the value observed on the starting material. The very low σ_b and ε_b values found for fully substituted QXS sample may

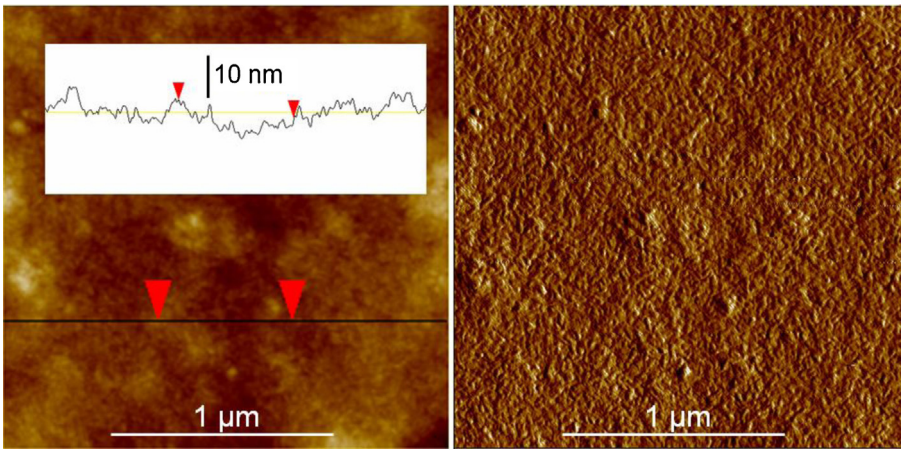

Fig. 2. AFM height and phase images of film prepared from sonicated xylan.

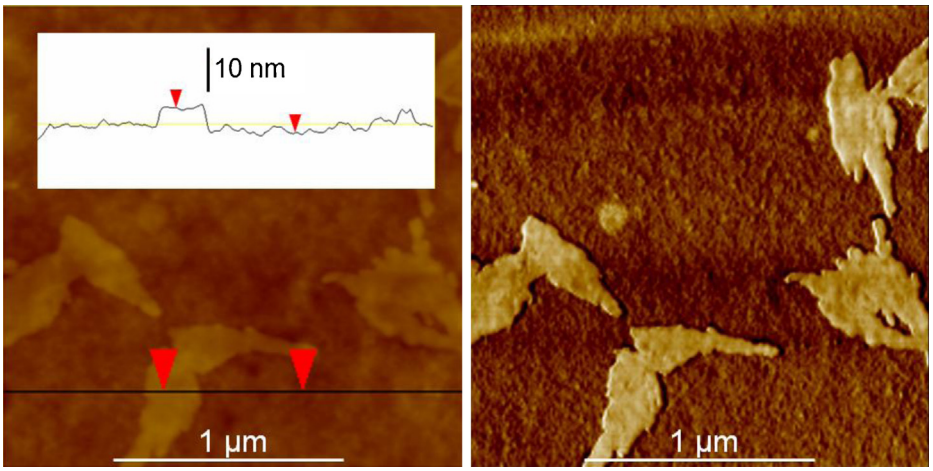

Fig. 3. AFM height and phase images of QX film.

indicate that the elongation at break is dependent on the amount of unsubstituted hydroxyls which provide the hydrogen bonding effect. More important (dominating) effects seem to be the above mentioned irregular structure (Fig. 6b) together with significant interaction of oppositely charged groups resulting in ionic linking as indicated by M_n values (Table 2).

On the other hand, SXQ leads to higher and better balanced mechanical behavior in comparison with opposite order of modification, exceeding that of QX sample. Generally, the level of mechanical parameters of all samples is still relatively good and comparable with many "commodity" polymers. Moreover, it exceeds parameters of many polysaccharide-based materials, like those obtained on branched arabinoxylan reinforced with cellulose fibrils (Mikkonen et al., 2012). The tensile strength of X is higher than the value determined on arabinoxylan (AX) reinforced with microfibrillated cellulose, but the values of elongation at break were bigger on AX films. Also AX from rye flour or wheat grain exhibited less attractive mechanical properties than X used in our studies (Hoije, Sternemalm, Heikkinen, Tenkanen, & Gatenholm, 2008; Ying et al., 2013). Corn hull AX values of tensile strength and modulus were also lower than for X with elongation at 6–12% (Zhang & Whistler, 2004). The values were also comparable with birch xylan films and films prepared from wood hydrolysates enforced with carboxymethyl cellulose (Yaich, Edlund, & Albertsson, 2012).

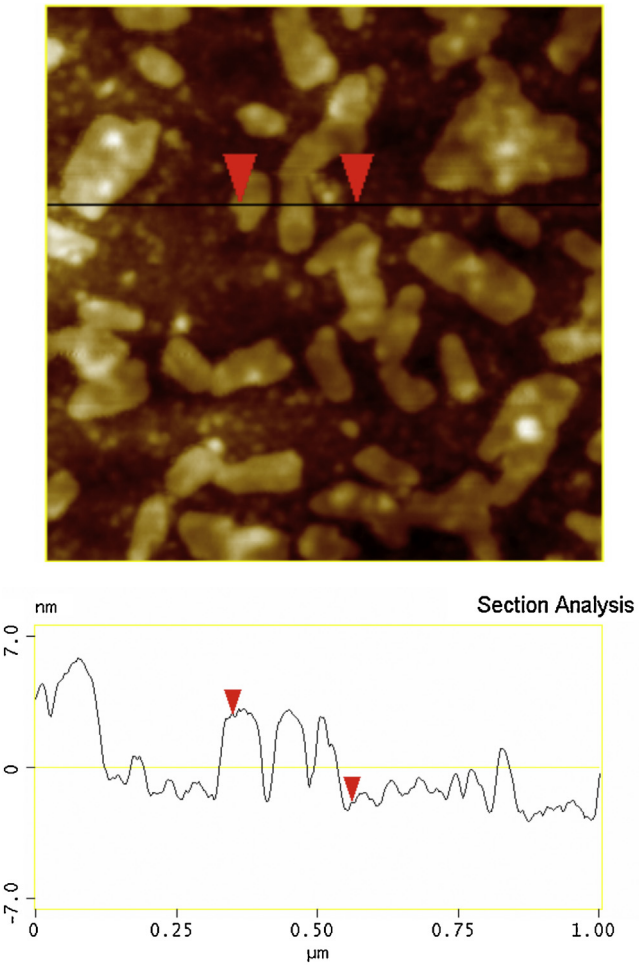

Fig. 4. AFM height and phase images of XS film.

3.5. XRD and solid state NMR analysis

As could be seen on Fig. 7a the XRD profile intensities of individual samples are decreasing in order X > XS > QXS > QX > SXQ. X and XS profiles have similar shape with broad peaks at $2\theta = 12.0$, 19.6, 20.8, 22.7 and 31.9° respectively. The remaining three profiles are much less intense and their structure could be considered as close to amorphous. It implies poor crystallinity of these films and indicates that the quaternization under alkaline conditions reduces the amount of the crystalline part. The five peak values listed above are close to data published on beech xylans with different 4-O-methyl-D-glucuronic acid content (Horio & Imamura, 1964). According to these authors, with increasing 4-O-methyl-D-glucuronic acid content the intensity of signals decreased and peaks were also shifted. Two other references (Gabrielli, Gatenholm, Glasser, Jain, & Keune, 2000; Grondahl et al., 2004) studied aspen wood xylan, which is according to the NMR data identical to 4-O-methyl-D-glucurono-D-xylan as from beech. Their listed WAXS profiles are also similar like ours. The data listed by other authors are differing probably

Table 3
Mechanical properties of studied xylan films.

Sample	E (MPa)	Thickness (mm)	σ_b (MPa)	ε_b (%)
X	7354 ± 383	0.05	108 ± 18	3.90 ± 0.95
XS	3530 ± 320	0.08	41.5 ± 4.5	1.60 ± 0.4
SX	3070 ± 245	0.20	60.0 ± 2	3.40 ± 0.3
SXQ	3650 ± 340	0.09	58.7 ± 6.5	2.55 ± 0.7
QX	2410 ± 135	0.35	57 ± 1.5	5.30 ± 1.0
QXS	3800 ± 800	0.08	17 ± 4	0.50 ± 0.04

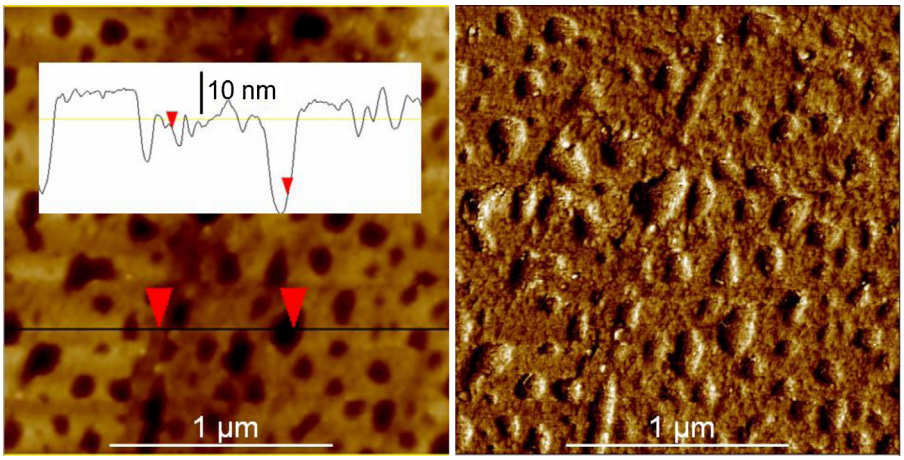

Fig. 5. AFM height and phase images of SX film.

due to different xylan sources (Lahaye, Rondeau-Mouro, Deniaud, & Buléon, 2003). All the above mentioned authors consider the source of crystallinity to be related to xylan referring to early results by Marchessault (Nieduszynski & Marchessault, 1972). They all ignore the possibility of the main source of crystalline structure in plants which is cellulose. This fact is also supported by new reviewed data showing XRD profiles close to our resulting from mercerization of cellulose I (Šimkovic, 2013). That is why we decided to run the solid state ^{13}C NMR spectrum of our xylan sample (X) to see if there are indications of cellulose presence.

The spectrum on Fig. 7b shows main xylan signals with peaks at 111.50 (teflon component of sample rotor), 102.143 (C-1), 74.384 (C-2 and C-3), and 64.220 (C-5) ppm. These chemical shifts are almost identical with our data obtained by solution NMR (Šimkovic et al., 2011a). According to solid state NMR results on xylan from other sources (Lahaye et al., 2003) the signals of solid/dry form are also close to our data with additional assignment of C-4 at 80–82 ppm, which is also a visible shoulder in our spectrum.

But additionally our spectrum has a broad overlapping part from 80 to 100 ppm where there is a peak at 88.77 ppm. This peak is indicative for cellulose C-4 signal when determining crystallinity by solid state ^{13}C NMR spectroscopy (Park, Baker, Himmel, Parilla, & Johnson, 2010). Additional cellulose signals known from literature could not be assigned probably due to low cellulose concentration and overlapping of cellulose and xylan signals (Pu, Ziemer, & Ragauskas, 2006). The peak at 88.77 ppm was also not observed in our solution ^{13}C NMR spectra. There is a peak at 90.1 ppm listed for C-3 of (1 → 3)-linked xylan listed in literature, but this is not a case of beech xylan (Lahaye et al., 2003). That is why we think that the insoluble particles observed in our films are related to cellulose crystalline and amorphous forms.

3.6. Thermal stability

According to TG/DTG/DTA analysis in air environment the onset temperature of X, indicating the start of the thermal degradation of the film is at 205 °C. The first DTA and DTG maxima (Table 4) are at an identical temperature (257 °C) when the maximal speed of degradation reaches 2.55 mg/min. At 300 °C the residue is slightly bigger than for xylan extracted from holocellulose with 5% NaOH (Šimkovic et al., 2011a). This indicates on increased presence of cellulose in the sample. The subsequent DTA and DTG peaks are indicating further carbonization and gasification processes at higher temperatures and the residue at 1000 °C is 4%, which is related to sodium salt of 4-O-methyl-D-glucuronic acid.

The partially sulfated sample SX has onset temperature at 184 °C, which is lower than for X as well as the DTG maximum at 250 °C. The first DTA peak is at 265 °C, which is slightly higher than

Table 4
TG/DTG/DTA data of studied films.

Sample	OT[a]	DTA peaks		DTG peaks		Residue [%] at [°C]				
	[°C]	[°C]	Δ [K/mg]	[°C]	[mg/min]	200	300	400	500	1000
X	205	257	0.0596	257	2.55	88	44	36	28	4
		289	0.0665	553	0.54					
		608	0.1678							
		793	0.0363							
SX	184	265	0.0463	250	2.64	86	47	37	24	9
		431	0.0652	478	0.58					
		506	0.1670	588	0.38					
		577	0.1775							
SXQ	201	276	0.0546	271	3.61	88	50	32	12	2
		402	0.0922	293	0.97					
		500	0.0870	492	0.85					
QXS	189	222	0.0029	218	3.56	87	55	38	27	24
		354	0.1071	319	1.08					
		482	0.1133	475	0.43					
		567	0.0137	565	0.10					

[a] Onset temperature.

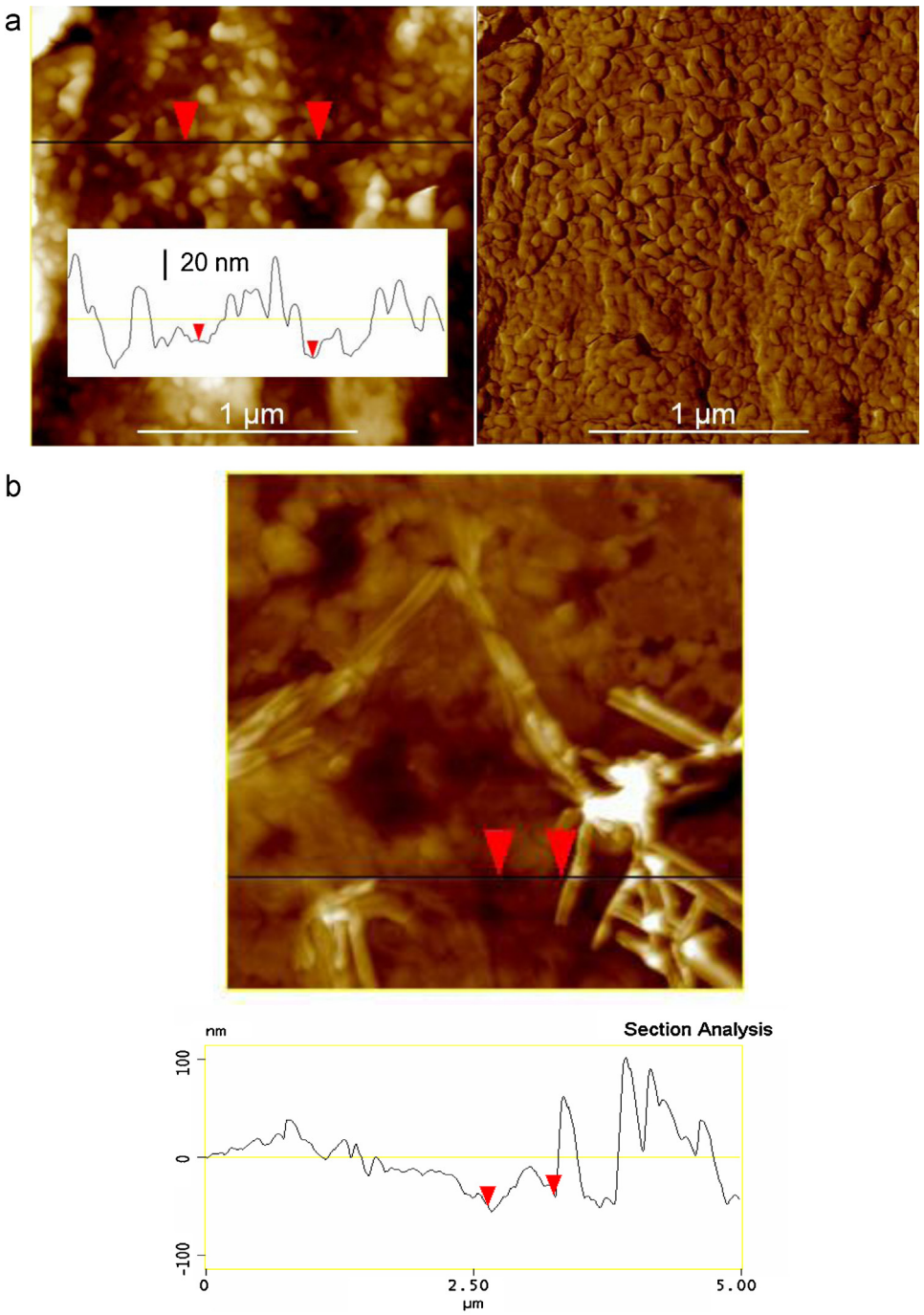

Fig. 6. AFM height and phase images of SXQ film (a) and QXS film (b).

for X and might be due to increased production of gaseus products due to the presence of sulfate groups. There are also three additional DTA peaks at 431, 506 and 577 °C as well as DTG peaks at 478 and 588 °C with 9% residue at 1000 °C. This sample is more stable than the sulfated films prepared before (Šimkovic et al., 2011b). It is probably due to the fact that SX has lower DS of sulfation than water soluble SX prepared at different reaction conditions. Their residues at 1000 °C indicated high salt content (9%) while the SX in the present study contains 11.31% of sodium. This was calculated from the sulphur content of anhydroxylose unit with $DS_S = 0.7$ ($M = 203$). It indicates that part of the sulfate groups were recycled into the acidic form during the thermal treatment and also might be affected by the presence of cellulose sulfate.

The SXQ sample prepared from SX by subsequent quaternization has onset temperature at 201 °C, which is higher than for SX. Also the first DTA and DTG peaks are shifted to higher temperatures in comparison with SX and X. The maximal rate of degradation at DTG peak (3.61 mg/min) is also higher than for SX and X and also the residue at 300 °C is bigger than for the two previous samples. In comparison with previous results on quaternized xylan films it is evident that the combined derivetive is more thermally stable with bigger residues and first DTA and DTG peks at higher

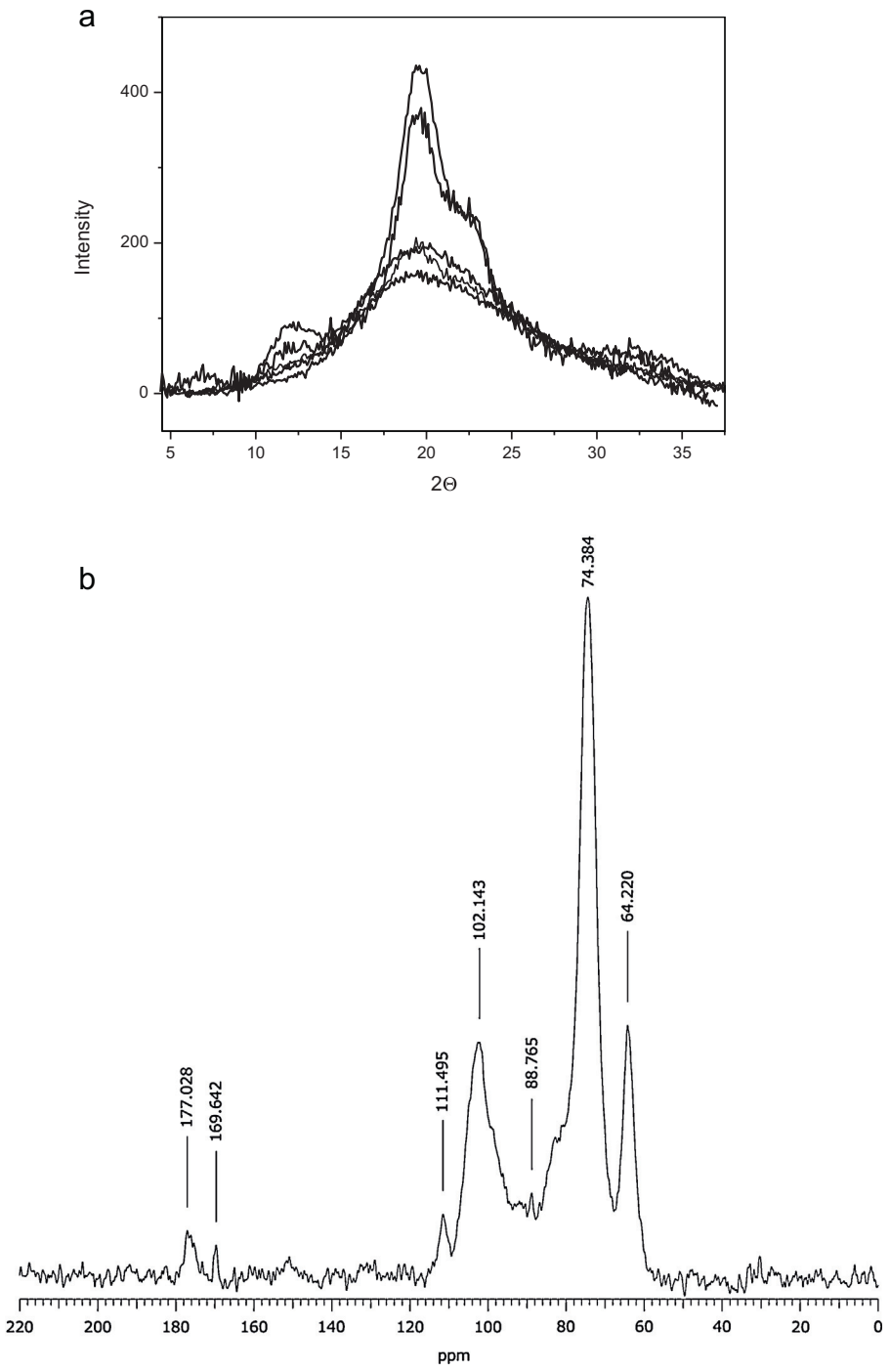

Fig. 7. WAXS profiles of studied samples with in order from the top: X > XS > QXS > QX > SXQ (a) and solid state ^{13}C NMR spectrum of X (b).

temperatures. The residue at 1000 °C indicates that the oppositely charged ion-exchanging groups are ionically bonded to each-other as the residue is only 2%. According to the sulfur and nitrogen content the sodium content of the corresponding anhydroxylose unit (M = 239) should be 9.63% and the presence of sulfated cellulose impurities were not taken into account.

For the QXS sample the thermal degradation started at 189 °C with first DTA and DTG maxima at 222 and 218 °C. These are much lower temperatures than observed on SXQ, SX and X. The shape of the TG curve is similar up to 200 °C as for SXQ. At higher temperatures the residue is bigger with values of 55, 38, 27 and 24% at 300, 400, 500 and 1000 °C. According to the calculated sodium content it should be only 6.64% at 1000 °C when the presence of sulfate cellulose was not taken into account. It could be concluded that the presence of cellulose affects the properties of this sample more dramatically than of the previus three. There are three additional DTA and DTG peaks (Table 4), which indicate more complicated thermal degradation processes than for SXQ.

4. Conclusions

Mechanical properties of all modified samples were reduced in comparison with X, but their level was still satisfactory and comparable with results on unmodified xylans from other sources.

Moreover the mechanical performance of SXQ was better balanced in comparison with that of SX and QX. The significantly reduced elongation of QXS sample indicated that this order of modification procedure caused embrittlement. It might be related to unfavorable high extent of interactions between oppositely charged groups. Both QXS and SXQ have higher onset temperatures than SX.

All the prepared films contain insoluble impurities. They are visible on the surface of the specimen when analyzed by AFM and according to maximal vertical surface differences the smoothness of the surface is increasing in order: X = QXS (∼100 nm) < SXQ (∼50 nm) < SX (∼20 nm) < XS = QX (∼10 nm). On the basis of XRD, SEC-MALS, AFM and both solution and solid state NMR we think that the insoluble components are cellulose impurities eluted with xylan by the alkaline extraction from beech wood. They probably also affect the mechanical properties of the specimens.

Acknowledgements

The authors are pleased to acknowledge the Polish-Slovak joint research project for years 2010–2012 period, entitled: "The study of polysaccharide films structure with the help of atomic force microscopy" and Lukasz Pietrzak for technical assistance; the State programs # 2003SP200280203 and 2003SP200280301 and Viktor Hronský for setting the conditions of the solid state NMR experiment; Slovak Granting Agency VEGA (Project No 2/7030/7, 2/0087/11 and 2/0007/13) for the support. Eva Špyrková is aknowledged for runing the TG/DTG/DTA experiments.

References

Deutschmann, R., & Dekker, R. F. H. (2012). From plant biomass to bio-based chemicals: Latest developments in xylan research. *Biotechnology Advances*, *30*, 1627–1640.

Ebringerova, A., Kramar, A., & Domanský, R. (1969). Structural features of (4-O-methylglucurono)xylan from wood of hornbean (*Carpinus butulus* L.). *Holzforschung*, *23*, 89–92.

Gabrielli, I., Gatenholm, P., Glasser, W. G., Jain, R. K., & Keune, L. (2000). Separation, characterization and hydrogel formation of hemicellulose from aspen wood. *Carbohydrate Polymers*, *43*, 367–374.

Grondahl, M., Eriksson, L., & Gatenholm, P. (2004). Material properties of plasticized hardwood xylans for potential application as oxygen barrier films. *Biomacromolecules*, *5*, 1528–1535.

Hansen, N. M. L., & Plackett, D. (2008). Sustainable films and coatings from hemicellulose: A review. *Biomacromolecules*, *9*, 1477–1505.

Hoije, A., Sternemalm, E., Heikkinen, S., Tenkanen, M., & Gatenholm, P. (2008). Materials properties of films from enzymatically tailored arabinoxylans. *Biomacromolecules*, *9*, 2042–2047.

Horio, M., & Imamura, R. (1964). Crystallographic study of xylan from wood. *Journal of Polymer Science Part A*, *2*, 627–644.

Lahaye, M., Rondeau-Mouro, C., Deniaud, E., & Buléon, A. (2003). Solid-state ^{13}C NMR spectroscopy of xylans in the cell wall of *Palmaria palmota* (L. Kuntze, Rhodophyta). *Carbohydrate Research*, *338*, 1550–1569.

Mikkonen, K. S., Pitkanen, L., Liljestrom, V., Bergstrom, E. M., Serimaa, R., Salmen, L., et al. (2012). Arabinoxylan structure affects the reinforcement of films by microfibrillated cellulose. *Cellulose*, *19*, 467–480.

Nieduszynski, I. A., & Marchessault, R. H. (1972). Structure of β, D(1 → 4′)-xylan hydrate. *Biomacromolecules*, *11*, 1335–1344.

Park, S., Baker, J. O., Himmel, M. E., Parilla, P. P., & Johnson, D. K. (2010). Cellulose crystallinity index: Measurement techniques and their impact on interpreting cellulase performance. *Biotechnology for Biofuels*, *3*, 10.

Peng, X., Ren, J., Zhang, L., & Sun, R. (2011). Nanocomposite films based on xylan-rich hemicelluloses and cellulose nanofibers with enhanced mechanical properties. *Biomacromolecules*, *12*, 3321–3329.

Pu, Y., Ziemer, C., & Ragauskas, A. J. (2006). CP/MAS ^{13}C NMR analysis of cellulase treated bleached softwood kraft pulp. *Carbohydrate Research*, *341*, 591–597.

Šimkovic, I. (2008). What could be greener than composites made from polysaccharides? *Carbohydrate Polymers*, *74*, 759–762.

Šimkovic, I. (2013). Unexplored possibilities of all-polysaccharide composites. *Carbohydrate Polymers*, *95*, 697–715.

Šimkovic, I., Gedeon, O., Uhliariková, I., Mendichi, R., & Kirschnerová, S. (2011a). Positively and negatively charged xylan films. *Carbohydrate Polymers*, *83*, 769–775.

Šimkovic, I., Gedeon, O., Uhliariková, I., Mendichi, R., & Kirschnerová, S. (2011b). Xylan sulphate films. *Carbohydrate Polymers*, *86*, 214–218.

Wang, Z. M., Li, L., Zheng, B. S., Normakhamatov, N., & Guo, S. Y. (2007). Preparation and anticoagulation activity of sodium cellulose sulfate. *International Journal of Biological Macromolecules*, *41*, 376–382.

Yaich, A. I., Edlund, U., & Albertsson, A.-C. (2012). Wood hydrolysate barriers: Performance controlled via selective recovery. *Biomacromolecules*, *13*, 466–473.

Zhang, P., & Whistler, R. L. (2004). Mechanical properties and water vapor permeability of thin film from corn hull arabinoxylan. *Journal of Applied Polymer Science*, *93*, 2896–2902.

Ying, R., Rondeau-Mouro, Barron, C., Mabille, F., Perronnet, A., & Saulinier, L. (2013). Hydration and mechanical properties of arabinoxylans and β-D-glucans films. *Carbohydrate Polymers*, *96*, 31–38.